arXiv:1802.06914

A BINARY OFFSET EFFECT IN CCD READOUT AND ITS IMPACT ON ASTRONOMICAL DATA

K. Boone,[1,2] G. Aldering,[1] Y. Copin,[3] S. Dixon,[1,2] R. S. Domagalski,[1,4,5] E. Gangler,[6] E. Pecontal,[7] and S. Perlmutter[1,2]

[1]*Physics Division, Lawrence Berkeley National Laboratory, 1 Cyclotron Road, Berkeley, CA, 94720*
[2]*Department of Physics, University of California Berkeley, 366 LeConte Hall MC 7300, Berkeley, CA, 94720-7300*
[3]*Université de Lyon, F-69622, Lyon, France ; Université de Lyon 1, Villeurbanne ; CNRS/IN2P3, Institu de Physique Nucléaire de Lyon*
[4]*Department of Astronomy, University of Toronto, 50 St. George St., Toronto, ON, M5S 3H4, Canada*
[5]*Dunlap Institute for Astronomy & Astrophysics, 50 St. George St., Toronto, ON, M5S 3H4, Canada*
[6]*Laboratoire de Physique Corpusculaire de Clermont-Ferrand, F-63171 Aubiere Cedex, France*
[7]*Centre de Recherche Astronomique de Lyon, Université Lyon 1, 9 Avenue Charles André, F-69561 Saint Genis Laval Cedex, France*

"Binary Offset"
-UH88/SNIFS
- 下図の右側の領域（読み出しチャンネル）では、高い値のピクセル直後に読みだされた値が~1ADU小さくなっている？

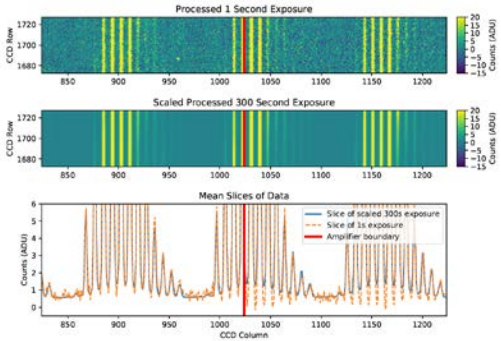

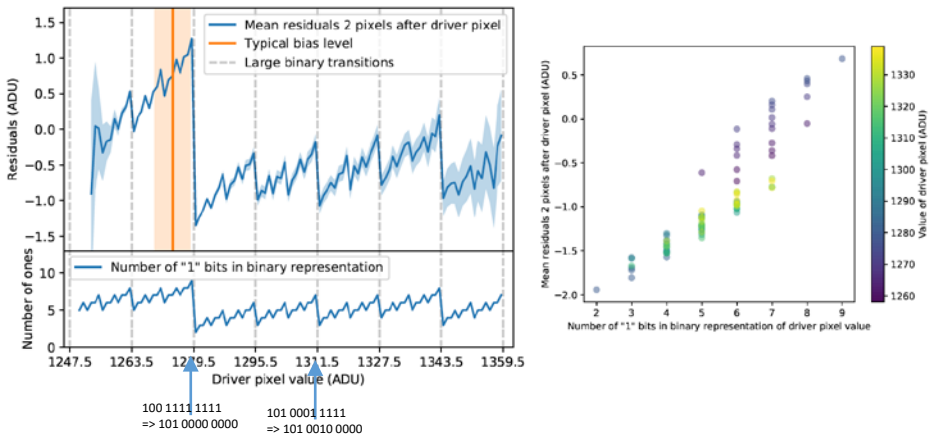

二つ前のピクセルの読み出し値の2進数表現で、"1"の数が多いほどオフセットが大きい？

フラットに最大で4.2%のシステマティック・オフセットが入る

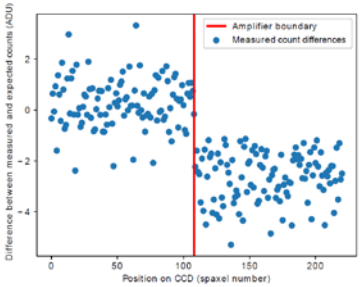

Figure 5. Exposure-time normalized difference between extracted 1 second and 300 second dome flats from the SNIFS blue channel, illustrating the "blue step". Each point corresponds to the average flux of a spaxel in the 4000 to 4500 Å region. We indicate the boundary where the readout switches from the left to the right amplifier with a vertical red line. We find a 2.2 ADU difference in the measured fluxes between the two amplifiers which corresponds to a 4.2% difference in the measured flux for this example.

原因はおそらく、ADCのreference voltageに出力が影響している
(16bitだと、1bitが0.0015%)
=> オフセットは使っているADCに依存する。

Telescope	Instrument	Distance from driver pixel to target pixel (pixels)	Approximate peak-to-peak amplitude of binary offset effect (ADU)	Amplitude in electrons	CCD front end	ADC	Reference
Blanco	DECam	-	Not detected (< 0.05)	Not detected (< 0.2)	Monsoon	Analog Devices AD7674	Castilla et al. (2010)
CFHT	Megacam	1	0.4	0.6		Linear Technology LTC 1604	de Kat et al. (2004)
Gemini	GMOS-S E2V	2, 3	0.7	1.4	ARC Gen. II	Datel ADS-937	Hook et al. (2004)
	GMOS-S Hamamatsu	-	Not detected (< 0.05)	Not detected (< 0.08)	ARC Gen. III		Gimeno et al. (2016)
	GMOS-N E2V	2, 3	0.7	1.4	ARC Gen. II	Datel ADS-937	Hook et al. (2004)
	GMOS-N Hamamatsu	-	Not detected (< 0.05)	Not detected (< 0.09)	ARC Gen. III		Gimeno et al. (2016)
HST	WFC3 UVIS	1	0.05-0.15[a]	0.08-0.23[a]			
	STIS (post SM4)	1	0.5-4.5[a]	0.5-4.5[a]			
	ACS	1, 2, 3, 4	0.4-1.0[a]	0.4-1.0[a]			
Keck	DEIMOS	2	2.6	3.2	ARC Gen. II	Datel ADS-937	Wright et al. (2003)
	HIRES	2	0.3	0.6	ARC Gen. I	Datel ADS-937	Kibrick et al. (1993)
	LRIS B	2	0.15	0.24	ARC Gen. I	Datel ADS-937	McCarthy et al. (1998)
	LRIS R (upgraded)	2	0.15	0.15	ARC Gen. II	Datel ADS-937	Rockosi et al. (2010)
SDSS	-	-	Not detected (< 0.05)	Not detected (< 0.23)		Crystal Semiconductor CS5101A	Gunn et al. (1998)
Subaru	Suprime-Cam	-	Not detected (< 0.05)	Not detected (< 0.15)	MFront	Analogic ADC423	Miyazaki et al. (2002)
	Hyper Suprime-Cam	1	0.5[b]	1.6[b]	MFront2	Analog Devices AD7686C	Nakaya et al. (2012)
	FOCAS	2	0.1[b]	0.2[b]	MFront	Analogic ADC423	Kashikawa et al. (2002)
UH88	SNIFS blue channel	2, 3	2.4	1.8	ARC-41 Gen. II	Datel ADS-937	Aldering et al. (2002)
	SNIFS red channel	2, 3	1.5	1.1	ARC-41 Gen. II	Datel ADS-937	Aldering et al. (2002)
VLT	FORS 1	1	0.1	0.22	FIERA	Analogic ADC4320A[c]	Beletic et al. (1998)
	FORS 2	1	0.1	0.13	FIERA	Analogic ADC4320A[c]	Beletic et al. (1998)
	MUSE	-	Not detected (< 0.05)	Not detected (< 0.06)	NGC	Analog Devices AD7677[c]	Reiss et al. (2012)

モデル化して補正することが可能。
SNIFSでは実装済み